Light Scattering by Gold Nanoparticles: Role of Simple Dielectric Models

Samantha Bruzzone,* Marco Malvaldi, Giovanni P. Arrighini, and Carla Guidotti

Dipartimento di Chimica e Chimica Industriale, Università di Pisa,Via Risorgimento 35, 56125 Pisa, Italia

Received: February 10, 2004; In Final Form: May 10, 2004

Near-field and far-field extinction and scattering efficiencies for UV−vis-irradiated spherical gold nanoparticles of varying size have been estimated as a function of the radiation wavelength. Several different dielectric function models are used to explore the role of quantum-size effects. The results suggest that the utilization of bulk dielectric data does not capture quantitatively important size effects and may correspond to an unjustified oversimplification.

I. Introduction

The study of the interaction of light with metallic nanoparticles and nanoparticle aggregates is fundamental to modern pure and applied research, in particular the development of a variety of spectroscopies and microscopies (surface-enhanced Raman scattering (SERS),[1] single-molecule detection,[2] near-field scanning methodologies,[3] etc.). The fact that nanoparticles are capable of generating local fields much more intense than the externally applied field and the marked dependence of these local fields on both shape and size of the scattering particle as well as the nature of the surrounding medium have promoted widespread use of metallic particles as chemical sensors[4] and photonic devices.[5] For what concerns surface enhanced spectroscopy (SES), it is commonly accepted that the basic phenomena are originated from both electromagnetic (e.m.) and chemical effects, simultaneously.[1] The debate on the relative importance of the two effects is not yet completely settled. The exceptional quantity of available data collected under many different experimental conditions are often difficult to compare, being sometimes even discordant, does not favor further insight into the matter. A number of parameters (for example, surface roughness, substrate/molecule electronic interactions, linear and nonlinear superimposed optical effects, pH, and solvents) can influence heavily the results. All of this considered, indubitable order-of-magnitude assessment of the response enhancement and even the very reproducibility of experiments in SES phenomena are still a fairly distant target to be reached.

A sizable number of both experimental and theoretical works[6−9] have investigated the far-field scattering by nanoparticles as well as short-distance interactions involved in SES as probed by scattered fields near the surface of the particle.[10,11] The far-field response corresponds to transverse outgoing e.m. waves, while the electric field near the surface of a perfect, spherical conductor must be normal to the surface. In a region sufficiently close to the sphere, the outgoing field has a nonnegligible radial component, which is distorted compared to the far field, to satisfy the boundary conditions.[12] Mie theory[13] allows one to calculate the scattering efficiency, Q_{sca}, far from the irradiated particle. The complete analytical solution based on the expansion of incident, propagating, and scattered fields in terms of vector spherical harmonics leads via Poynting theorem to the desired extinction and scattering efficiencies of the sphere. The approach provides general expressions for the scattered field and consequently solves the problem in the far-field region. No surprise, therefore, that the same treatment yields the near-field efficiencies, Q_{NF}.[14] From the point of view of both spectroscopic enhancement and long-range interactions between particles, it is interesting to note that Q_{sca} is independent of the distance to the surface of the scattering sphere while Q_{NF} has a distance dependence and is greater than Q_{sca}.[15]

The expressions for the efficiencies Q_{sca} and Q_{NF} depend on the dielectric function of the particle through its scattering coefficients.[12] In a lot of works concerning SES,[7,8] the scattering efficiencies have been calculated adopting, for the dielectric function of the nanosized cluster, experimental bulk dielectric data or, alternatively, an approximate estimate based on the free-electron Drude model.[15−17] It is well established[18] that the dielectric behavior of a very small particle depends on its size when the dimensions become comparable to or smaller than the bulk mean free electron path. To our knowledge, a systematic study to establish the influence of more realistic size-dependent dielectric models on near-field scattering properties has never appeared in the literature. In the present work, we compare the behavior of the scattering efficiencies Q_{sca} and Q_{NF} versus the wavelength of the incident field as the particle dimensions are varied by calculating the dielectric function of the nanoparticle as follows: (i) from experimental bulk refractive index data; (ii) according to Drude theory; (iii) with a simple quantum model for the electronic structure (free electrons in a box), which has been shown to reproduce satisfactorily some spectroscopic properties of metal clusters.[19−21]

In section II the models utilized will be briefly outlined, whereas numerical results and discussion are addressed to sections III and IV.

II. Dielectric Model

Q_{sca}, defined as the ratio between scattered and incident power for a given geometric cross-section, is a measure of the capability of a sphere to redirect the incident e.m. wave by scattering over all solid angle.[12] Analogously, the quantity defined as Q_{NF} represents the capability of the sphere to convert power from the incident field near the surface of the sphere and thus can be used to calculate the intensity of the electric field there. Following Quinten,[22] Q_{sca} and Q_{NF} can be expressed in the forms

* Corresponding author. Phone: +390502219294. Fax: +390502219260. E-mail: sama@dcci.unipi.it.

10.1021/jp049401h CCC: $27.50
Published on Web 06/19/2004

$$Q_{sca} = \frac{2}{(kR)^2}\sum_{n=1}^{\infty}(2n+1)(|a_n|^2 + |b_n|^2) \quad (1)$$

$$Q_{NF}(r) = 2\frac{r^2}{R^2}\sum_{n=1}^{\infty}\{|a_n|^2[(n+1)|h_{n-1}{}^{(1)}(kr)|^2 + n|h_{n+1}{}^{(1)}(kr)|^2] + (2n+1)|b_n|^2|h_n{}^{(1)}(kr)|^2\} \quad (2)$$

where R is the particle radius, $k = (2\pi n_0(\lambda))/\lambda$ is the wavenumber outside the particle, λ is the incident-field wavelength, and n_0 is the refractive index of the host matrix. $h_n{}^{(1)}$ is a spherical Hankel function of the first kind of order n, and a_n and b_n are scattering coefficients of the sphere whose simplified forms are[12]

$$a_n = \frac{m\psi_n(mx)\psi_{n'}(x) - \psi_n(x)\psi_{n'}(mx)}{m\psi_n(mx)\xi_{n'}(x) - \xi_n(x)\psi_{n'}(mx)} \quad (3)$$

$$b_n = \frac{\psi_n(mx)\psi_{n'}(x) - m\psi_n(x)\psi_{n'}(mx)}{\psi_n(mx)\xi_{n'}(x) - m\xi_n(x)\psi_{n'}(mx)} \quad (4)$$

Here m is the relative refractive index, i.e., the ratio between particle refractive index and n_0, and $x = kR$ is the size parameter. The functions $\xi_n(\rho)$ and $\psi_n(\rho)$ are the well-known Riccati−Bessel functions, $\psi_n(\rho) = \rho j_n(\rho)$ and $\xi_n(\rho) = \rho h_n{}^{(1)}(\rho)$, with $j_n(\rho)$ being the n-order spherical Bessel function. In the applications considered in this paper, the host matrix is the vacuum, so that $n_0 = 1$, whereas the dielectric function of the particle has been evaluated on the basis of the approximations described in the preceding section. The near-field efficiency $Q_{NF}(r)$ has been calculated on the surface of the particle ($r = R$).

As a consequence of the reduced dimensions of the particles considered, the electronic-band structure involved breaks up into discrete levels.[23] The simplest quantum model able to treat this situation is a delocalized, noninteracting electron gas confined by a box with impenetrable walls. The system is coupled to a positively charged background homogeneously distributed over the box volume to ensure electrical neutrality (jellium model).[19,24] This picture represents the hypothesis that the particle can be treated as a system of loosely bound electrons associated with the totality of the atoms aggregated to form the cluster. It has been shown that the role of the inner-shell electrons in noble metals cannot be ignored.[12,18,25] In particular, coin metals (Ag, Cu, Au) exhibit a rather complex behavior as a consequence of the strong coupling between the loosely bound conduction electrons of the s band and the localized electrons of the d band.[18,25,26] The presence of interband interactions can be satisfactorily approximated in terms of an additive complex contribution ϵ_{IB} to the dielectric function ϵ_{FE} associated with the delocalized electron gas. The imaginary part is not negligible only at frequencies where interband transitions occur, whereas the real part (often represented by a frequency-independent averaged value) is important also at lower frequencies. Accounting for the effects arising from free electron-inner electron interactions leads to a hybrid description of the involved electronic behavior.

The conduction-band electrons are represented in terms of the well-known eigenfunctions of the particle in a box. Despite the crudity of the model, this description allows the introduction of quantum-size effects in a natural way. The approach is able to deal with systems containing a large number of electrons without particular computational effort.[21] The number of free electrons in a particle of given size is calculated indirectly from the known expressions of the occupied energy levels, once the box size and the nature of the metal (through its Fermi energy, ϵ_F) have been fixed. Limiting ourselves to closed-shell configurations only, the number of electrons is twice the number of levels having energy lower than ϵ_F. The hybrid nature of the model is disclosed by the fact that the interband contribution ϵ_{IB} to the dielectric function is assumed to be independent of both particle size and wavelength. The value of ϵ_{IB} has been taken for gold to be 12 on the basis of experimental data.[27]

The volume of the cubic box is required to be equivalent to the volume of the corresponding spherical particle. The box edge is easily verified to be $L = (4\pi/3)^{1/3}R$.

On the basis of such considerations, the dielectric function can be expressed in the form[20,21]

$$\epsilon(\omega,R) = \epsilon_{IB}(\omega) + \epsilon_{FE}(\omega,R) \quad (5)$$

with

$$\epsilon_{FE}(\omega,R) = 1 + \frac{256L}{\pi^5 a_0}\sum_{mnp}\sum_{m'}\frac{f_{mnp}[1-(-1)^{m+m'}](mm')^2}{(m'^2-m^2)^3[(m'^2-m^2)^2 - x^2]} \quad (6)$$

where a_0 is the Bohr radius and f_{mnp} is the Fermi−Dirac occupation factor. The dimensionless quantity $x = 2ML^2\tilde{\omega}/\pi^2\hbar$, where $\tilde{\omega} = \omega + i\eta$, and ω is the angular frequency of the applied e.m. field. The limit $\eta \rightarrow 0^+$ is required by the assumption of infinitely slow switching-on of the e.m. interaction. The presence of the Fermi−Dirac occupation factor in eq 6 limits the sums over m,n,p to doubly occupied levels only, while through the unrestricted sum over m' the electromagnetic perturbation effects (polarization) are properly taken into account. In eq 5, the finite size of the particle appears explicitly, but additional implicit size effects arise from the sums over the states.

Below we briefly review the salient points of the Drude model. According to this venerable model, real and imaginary parts of the dielectric function can be expressed as follows[26]

$$\epsilon(\omega,R) = \epsilon_{IB} - \frac{\omega_p{}^2}{\omega(\omega + i\omega_d)} \quad (7)$$

where ω_p is the bulk plasma frequency, $\omega_p{}^2 = Ne^2/ML^3$, with N/L^3 the number density of free electrons in the bulk metal, M the electronic mass, and ω_d the damping frequency. ω_d depends on the mean free path l of the conduction electrons and the Fermi velocity v_F, $\omega_d = v_F/l$. If the radius R of the nanoparticle is smaller than the mean free path l, the conduction electrons are scattered by the particle surface and the mean free path l_{eff} becomes size-dependent according to the standard approximation $l_{eff}{}^{-1} = R^{-1} + l^{-1}$.[29] In this work, the parameters v_F and l_{eff} have been calculated from data given in ref 30. Bulk dielectric data has been taken from the early work of Johnson and Christy,[31] which is employed extensively even in recent works.[32]

The choice of the simple box model to describe the quantum-size effects inherent in the nanosized particle deserves a few comments. We are aware that dielectric results for a spherical particle can only imperfectly be mimicked by those deduced for a cubic box structure on the basis of the simple volume-equivalence requirement previously remarked (the dielectric response of small metal particles has been quantum-mechanically solved for many different geometric shapes, including the sphere[28]). Our primary intent in this paper, however, is to assess in near-field scattering calculations the prominence of quantum-

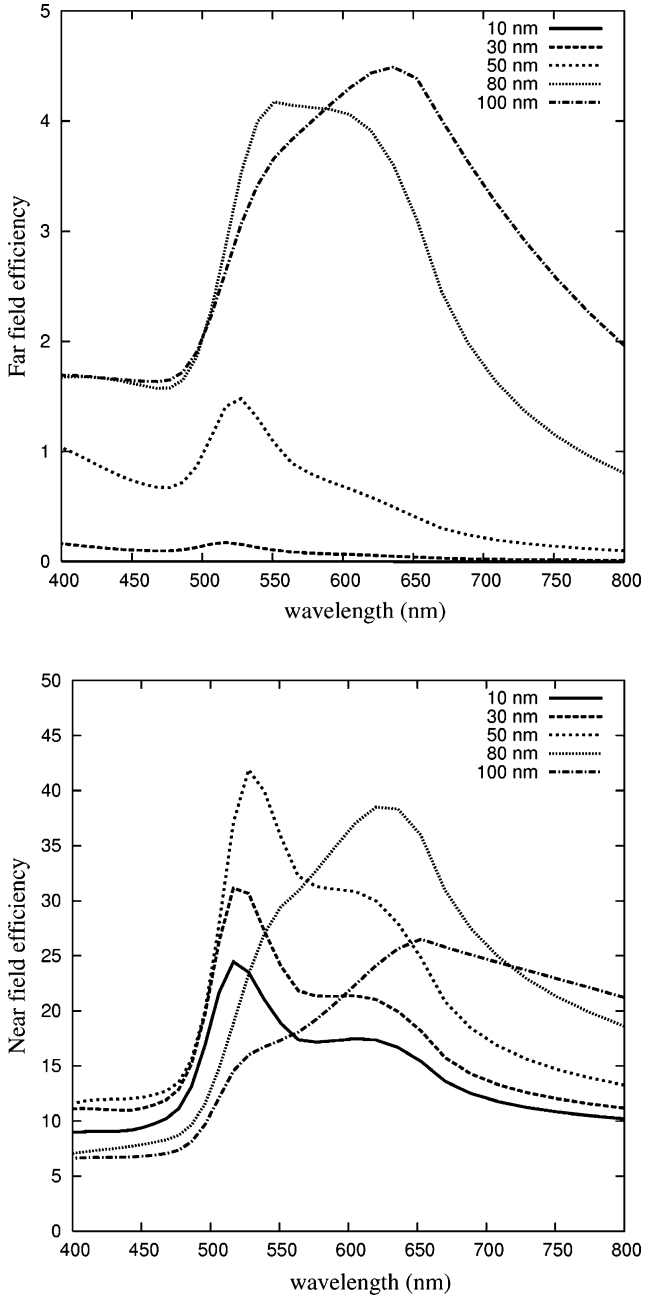

Figure 1. Efficiency vs optical wavelength for Au particles with different radius (10, 30, 50, 80, 100) obtained using bulk dielectric data:[30] (a) Far-field; (b)Near-field. Host medium: $\epsilon_m = 1$.

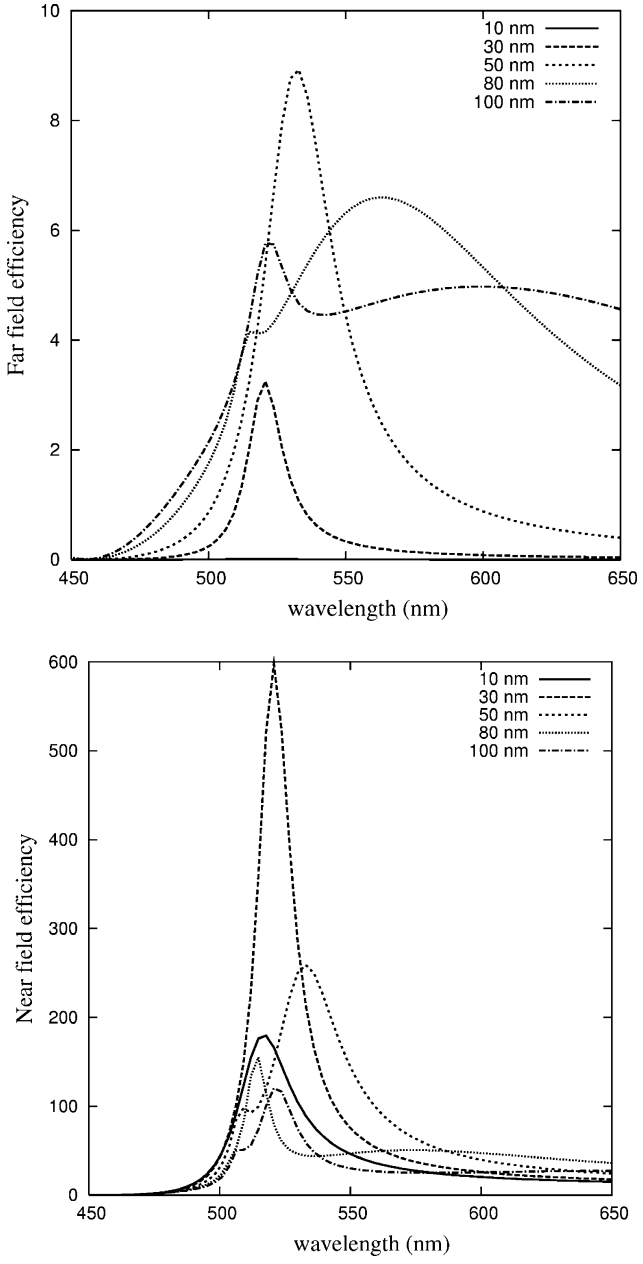

Figure 2. Efficiency vs optical wavelength for Au particles with different radius (10, 30, 50, 80, 100) obtained using a dielectric function calculated according to the Drude model: (a) Far-field; (b) Near-field. Host medium: $\epsilon_m = 1$.

size effects rather than their absolute magnitude. Considering that the crude model we are adopting has been shown to correctly reproduce experimental trends for nanosized particles of different shapes,[21] it seems reasonable to conjecture that at this level of investigation our treatment should be able to capture the essential physical features involved. As a final remark, it must be borne in mind that gold particles with a diameter of about 1 nm (and generally speaking the surface roughness responsible for SES effects) can hardly be regarded as perfect spheres and associated with a simple geometry.

III. Results

The particles studied in this work have a radius between 1 and 100 nm to include situations where quantum-size effects are not expected to be important as well as situations where they are expected to play a nonnegligible role. The range of dimensions chosen is also representative of the typical dimensions of particles or defects that are experimentally found to promote SERS.[1,4]

In Figure 1 the behavior of the efficiencies Q_{sca} and Q_{NF}, calculated according to eqs 1 and 2 using bulk dielectric data,[30] are reported as a function of the wavelength. Note that the Q_{sca} values for a particle with a 10 nm radius are quite small, so that the relative curve merges with the zero-valued axis in the figure. This happens not only for calculations with bulk dielectric data but even for all other calculations presented (see Figures 2 and 4). As already stressed by Quinten,[22] the smaller the radius of the particle, the larger the ratio Q_{NF}/Q_{sca}. In Figure 5a the values of the latter ratio are reported as a function of the wavelength for any radius considered.

In Figure 2, in an analogous fashion, the same quantities are reported and their ratio compared. In this case, Q_{sca} and Q_{NF} are still calculated using eqs 1 and 2 but the dielectric data is

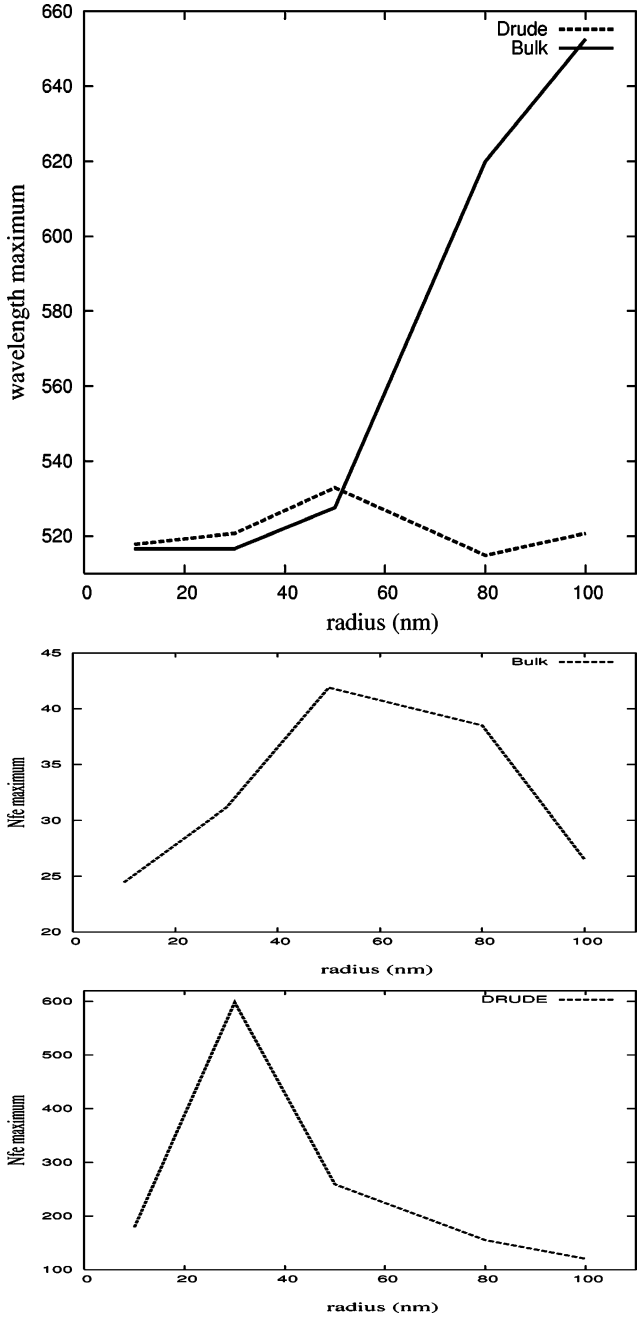

Figure 3. (a) Near-field scattering peak wavelength vs Au particle radius (10, 30, 50, 80, 100) according to the Drude model (solid line) and using bulk dielectric data[30] (dotted line). (b) Near-field efficiency maximum value vs Au particle radius (10, 30, 50, 80, 100) from bulk dielectric data[30] and (c) according to the Drude model. Host medium: $\epsilon_m = 1$.

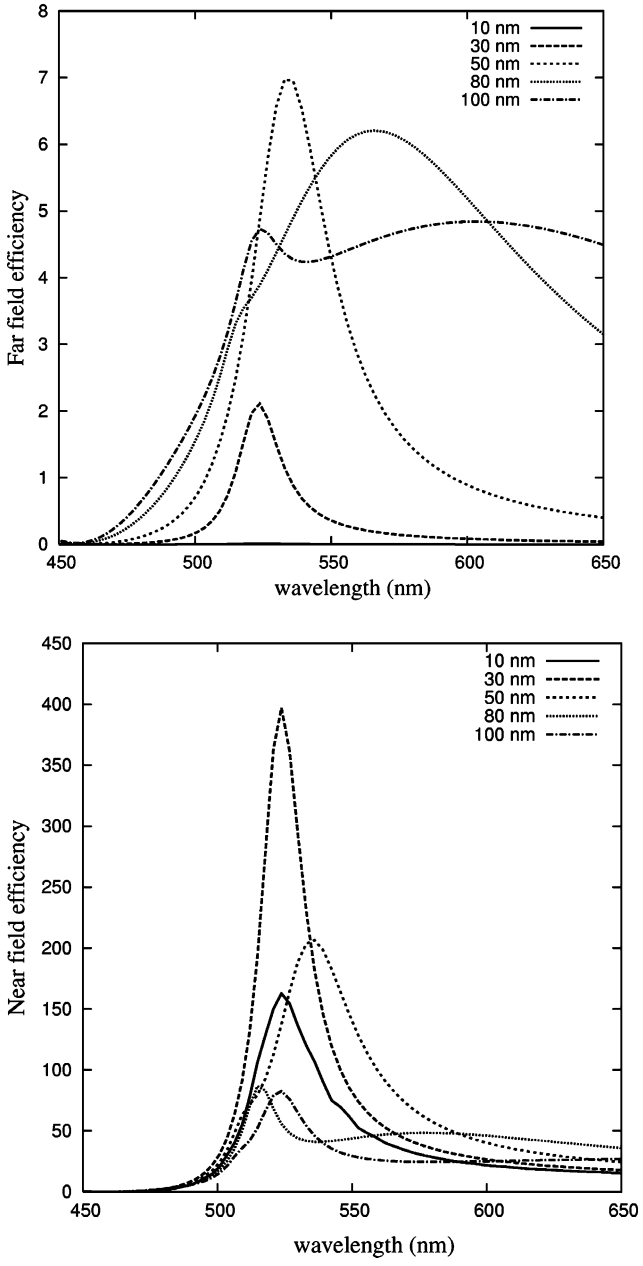

Figure 4. (a) Efficiency vs optical wavelength for Au particles of different radius (10, 30, 50, 80, 100) obtained from dielectric function data calculated according to the quantum box model: (a) Far-field; (b) Near-field. Host medium: $\epsilon_m = 1$.

deduced according to Drude, eq 7. Now the bandwidth appears noticeably reduced and the scattering efficiency is enhanced in both cases. The near-field efficiency is approximately 1 order-of-magnitude larger with respect to the former case. In addition, the maximum efficiency wavelengths are blue shifted and concentrated within a more limited range, lying between 500 and 550 nm (see Figure 3a). As one can observe in Figure 5b, the ratio Q_{NF}/Q_{sca} no longer monotonically rises with increasing wavelength and displays a shoulder slightly before 500 nm. Finally, the maximum intensity of Q_{NF}, calculated using bulk dielectric data (Figure 3b), increases as we move from a dimension of 10 to 50 nm, followed by decrease beyond this dimension. The peak intensity for Q_{NF} using the quantum box model (Figure 3c) reaches its maximum value for particles of about 30 nm and then decreases.

Figure 4 shows scattering efficiencies calculated by using dielectric function data obtained from the quantum box model (see eqs 5 and 6) for particles of the same dimensions considered previously. From a qualitative point of view, no important differences can be detected with respect to Figure 2. Clear differences, however, emerge for particles smaller than 10 nm (Figure 6). In this case, the quantum box model leads to well-defined fine structure related to single-electron excitations superimposing to form collective plasmon modes, something completely missing in the Drude model treatment. In Figure 7 a comparison of the results for the ratio Q_{NF}/Q_{sca} calculated according to the three dielectric models explored (bulk, Drude model, and quantum box model) is presented for a particle of radius 100 nm. We can see that the plots relative to the two calculations carried out in terms of size-dependent dielectric

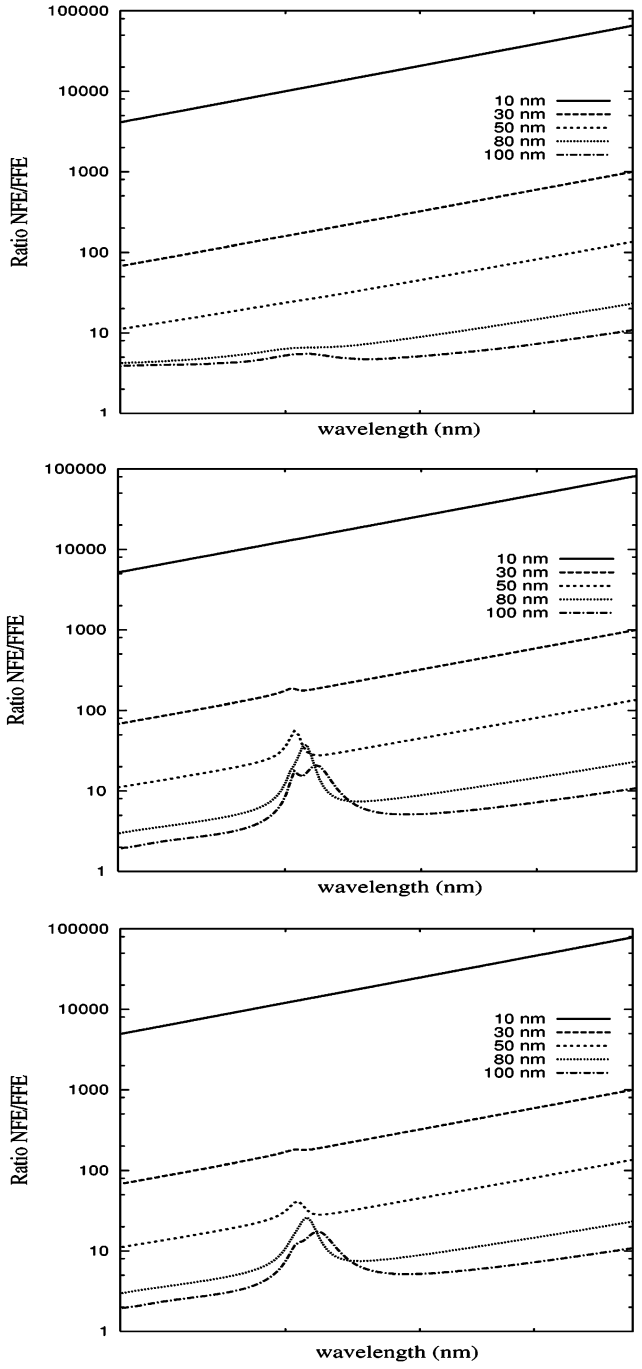

Figure 5. Ratio of the near-field to far-field scattering efficiency vs optical wavelength for Au particles of different radii (10, 30, 50, 80, 100) obtained (a) from bulk dielectric data,[30] (b) according to the Drude model, (c) according to the quantum box model.

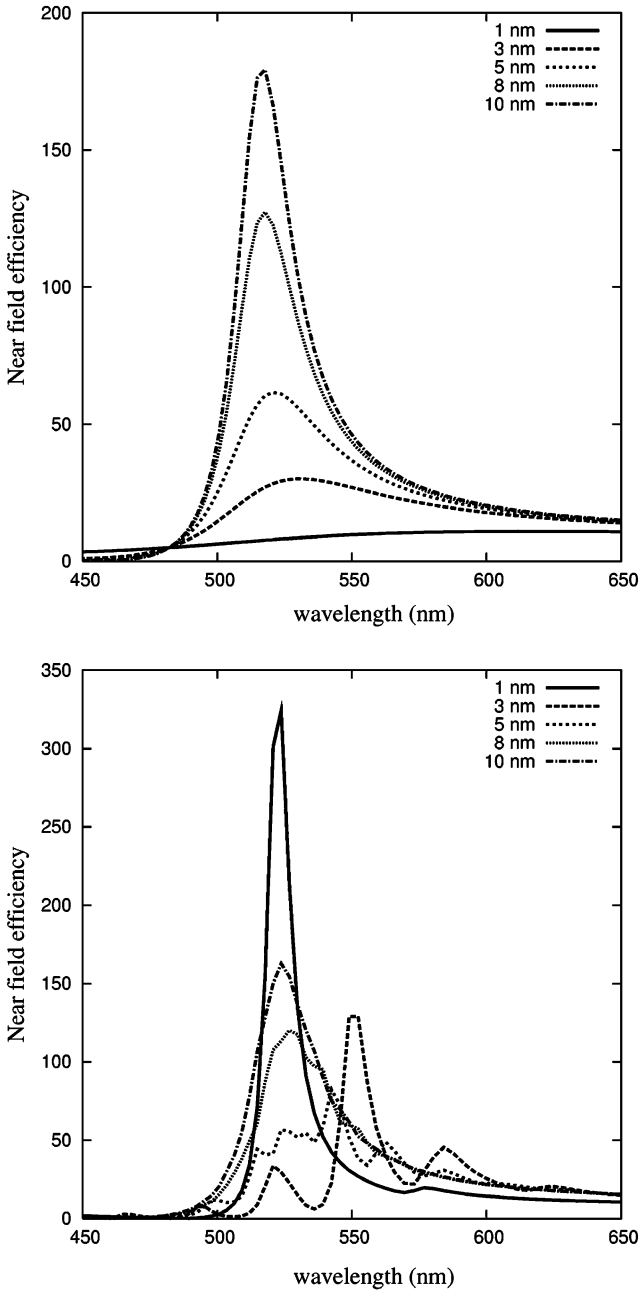

Figure 6. Near-field efficiency vs optical wavelength for Au particles of different radius (1, 3, 5, 8, 10) obtained from dielectric data calculated according to the (a) Drude model and (b) Quantum box model. Host medium: $\epsilon_m = 1$.

function data show a more intense peak than the plot obtained using the bulk dielectric function at the plasmon wavelength (520 nm), confirming that the size dependence of plasmon modes influences quantitatively the scattering phenomena.

IV. Conclusions

The semiempirical approach applied in this work to gold nanoparticles offers an easy and direct way to introduce quantum-size effects into the dielectric behavior. The understanding of electromagnetic phenomena involving small particles is believed to be of capital importance in unraveling many issues of surface-enhanced spectroscopies such as SERS.

Some qualitative and quantitative differences emerge from the introduction of size dependence in the dielectric behavior. From such differences it can be concluded that the absorption of light by a molecule near a nanometric metallic scattering center is strongly influenced by the dimension of the latter, not only through geometrical near-field enhancement, but also by virtue of the variation of the dielectric function related to dimensional features. It seems like reasonable speculation to suggest that quantitative predictions about enhancement factors in SERS can be hardly reconciled with use of bulk dielectric data for the metal nanoparticles involved.

The model used is surely not comprehensive of all the different effects that the particle size can induce on the dielectric behavior. In particular, the estimate of the damping effects and their size dependence, whose importance cannot be ignored in light−nanoparticle interactions,[33] is very rough, while the introduction of interband contributions deserves quite different attention. Moreover, if the particles embedded in the host

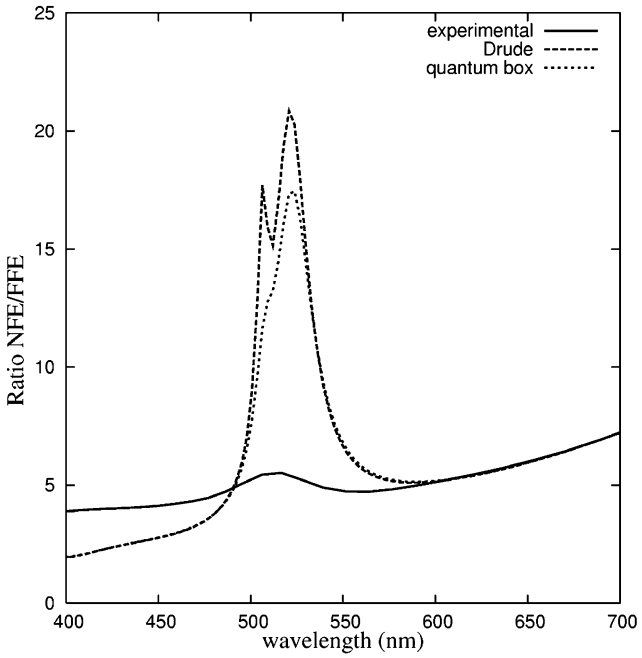

Figure 7. Ratio Q_{NF}/Q_{sca} vs optical wavelength for Au particles of $R = 100$ nm. Bulk dielectric data (full line), Drude dielectric model (thick dashed line), quantum box dielectric function (thin dashed line). Host medium: $\epsilon_m = 1$.

medium cannot be considered as infinitely diluted, a significant comparison with experiments cannot disregard the role of interparticle interactions.

Acknowledgment. Financial support by CNR (Progetto Finalizzato MSTA II) is gratefully recognized. M.M. was financially supported from the Istituto Nazionale di Fisica della Materia (INFM).

References and Notes

(1) Moskovits, M. *Rev. Mod. Phys.* **1985**, *57*, 783.
(2) Trautman, J. K.; Macklin, J. *J. Chem. Phys.* **1996**, *205*, 221.
(3) Dunn, R. C. *Chem. Rev.* **1999**, *99*, 2891.
(4) Elghanian, R.; Storhoff, J. J.; Mucic, R. C.; Letsinger R. L.; Mirkin, C. A. *Science* **1997**, *277*, 1078.
(5) Quinten, M.; Leitner, A.; Kren, J. R.; Aussenegg, F. R. *Opt. Lett.* **1998**, *23*, 1331.
(6) Else, J. M. *Waves Random Media* **1997**, *7*, 303.
(7) Barton, J. P. *Meas. Sci. Technol.* **1998**, *9*, 151.
(8) Vohnsen, B.; Bozhevolnyi, S. I. *Appl. Opt.* **2001**, *40*, 6081.
(9) Prodan, E.; Nordlander, P.; Halas, N. J. *Nano Lett.* **2003**, *3*, 1411.
(10) Wurtz, G. A.; Hranisavljevic, J.; Wiederrecht, G. P. *Nano Lett.* **2003**, *3*, 1511.
(11) Maier, S. A.; Brongersma, M. L.; Kik, P. G.; Atwater, H. A. *Phys. Rev. B* **2002**, *65*, 193408.
(12) Bohren, C. F.; Huffman, D. R. *Light scattering by small particles*; Wiley: New York, 1981.
(13) Mie, G. *Ann. Phys. (Leipzig)* **1998**, *25*, 377.
(14) Messinger, B. J.; von Raben, K. U.; Chang, R. K.; Barber, P. W. *Phys. Rev. B* **1981**, *24*, 649.
(15) Barber, P. W.; Chang, R. K.; Massoudi, H. *Phys. Rev. B* **1983**, *61*, 7251.
(16) Yang, W.-H.; Schatz, G. C.; Van Duyne, R. P. *J. Chem. Phys.* **1995**, *103*, 869.
(17) Schatz, G. C.; Van Duyne, R. P. Electromagnetic Mechanism of Surface-enhanced Spectroscopy. In *Handbook of vibrational Spectroscopy*; Wiley: Chichester, 2002.
(18) Kreibig, U.; Vollmer, M. *Optical Properties of metal clusters*; Springer-Verlag: Berlin, 1995.
(19) Genzel, L.; Martin, T. P.; Kreibig, U. *Z. Phys. B* **1975**, *21*, 339.
(20) Wood, D. M.; Ashcroft, N. W. *Phys. Rev. B* **1982**, *25*, 6255.
(21) Bruzzone, S.; Arrighini, G. P.; Guidotti, C. *Chem. Phys.* **2003**, *291*, 125.
(22) Quinten, M. *Z. Phys. D* **1995**, *35*, 217.
(23) Frohlich, H. *Physica* **1937**, *6*, 406.
(24) Cini, M.; Ascarelli, P. *J. Phys. F* **1974**, *4*, 1998.
(25) Abelés, F. *Optical Properties of Solids*; North-Holland: Amsterdam, 1972.
(26) Hummel, R. E. *Electronic Properties of Materials*, 3rd ed.; Springer: Berlin, 2001.
(27) Mulvaney, P. *Langmuir* **1996**, *12*, 788.
(28) Kraus, W. A.; Schatz, G. C. *J. Chem. Phys.* **1983**, *79*, 6130.
(29) Kreibig, U.; Fragstein, C. V. *Z. Phys.* **1969**, *224*, 307.
(30) Ashcroft, N. W.; Mermin, N. D. *Solid State Physics*, int. ed.; Harcourt: Orlando, FL, 1976.
(31) Johnson, P. B.; Christy, R. W. *Phys. Rev. B* **1972**, *6*, 4370.
(32) Moskovits, M.; Smovà-Sloufovà, I.; Vlckovà, B. *J. Chem. Phys.* **2002**, *116*, 10435.
(33) Soennichsen, C.; Franzl, T.; Wilk, T.; von Plessen, G.; Feldmann, J.; Wilson, O.; Mulvaney, P. *Phys. Rev. Lett.* **2002**, *88*, 077402/1.